

Scaling and Suppression of Anomalous Heating in Ion Traps

L. Deslauriers, S. Olmschenk, D. Stick, W. K. Hensinger, J. Sterk, and C. Monroe*

FOCUS Center and Department of Physics, University of Michigan, Ann Arbor, Michigan 48109, USA

(Received 31 January 2006; published 8 September 2006)

We measure and characterize anomalous motional heating of an atomic ion confined in the lowest quantum levels of a novel rf ion trap that features moveable electrodes. The scaling of heating with electrode proximity is measured, and when the electrodes are cooled from 300 to 150 K, the heating rate is suppressed by an order of magnitude. This provides direct evidence that anomalous motional heating of trapped ions stems from microscopic noisy potentials on the electrodes that are thermally driven. These observations are relevant to decoherence in quantum information processing schemes based on trapped ions and perhaps other charge-based quantum systems.

DOI: [10.1103/PhysRevLett.97.103007](https://doi.org/10.1103/PhysRevLett.97.103007)

PACS numbers: 32.80.Pj, 39.10.+j, 42.50.Vk

Trapped atomic ions are an unrivaled source of long-lived entangled quantum states for applications ranging from precision metrology [1,2] to fundamental studies of quantum nonlocality [3] and quantum information processing [4,5]. Internal electronic states of multiple ions can be entangled through a mutual coupling to quantum states of the collective motion of the ion crystal, following a number of quantum logic gate schemes [4,6]. These ideas have spawned a flood of recent experimental work, including the generation of particular entangled states of many ions [7] and the implementation of a variety of simple quantum information algorithms [8].

An important source of decoherence in these systems has proven to be the heating of trapped ion motion, thought to arise from noisy electrical potentials on the trap electrode surfaces [5,9–11]. This decoherence is expected to become even more debilitating as ion traps become weaker in order to support larger ion crystals [4] and allow shuttling of ions through complex and microscale electrode structures [12]. More broadly, the electrode surface noise giving rise to anomalous heating in ion traps may also be related to parasitic electrical noise observed in many condensed-matter quantum systems [13].

In this Letter, we present a controlled study of motional heating in a novel ion trap geometry that permits the spacing between the electrodes and the trapped ion to be adjusted *in situ*. The electrodes in this apparatus can also be cooled through contact with a liquid nitrogen reservoir. When the temperature of the electrodes is reduced from 300 to about 150 K, the anomalous heating rate of trapped ion motion drops by an order of magnitude or more, but is still higher than that expected from thermal Johnson noise in the electrical circuit feeding the electrodes. These observations provide direct evidence that anomalous heating of trapped ions indeed originates from microscopic “patch” potentials [14], whose fluctuations are thermally driven and can be significantly suppressed by modest cooling of the electrodes.

Single cadmium ions are confined in a rf trap formed by two opposed needle-tip electrodes in a vacuum chamber

[15], as depicted in Fig. 1. The tungsten electrodes are attached to axial translation stages, allowing the tip-to-tip separation $2z_0$ to be controllably varied over a wide range with micrometer resolution; coaxial alignment is provided by transverse translation stages. A common electrical potential $U_0 + V_0 \cos(\Omega t)$ with $\Omega/2\pi = 29$ MHz is applied to the electrodes with respect to a pair of recessed grounded sleeves surrounding the needles, as shown in Fig. 1. The potential is delivered through a dual (bifilar) helical rf resonator, allowing the two electrodes to be independently biased with a static potential difference δU_0 in order to compensate for any background axial static electric fields. Ions are loaded into the trap by photoionizing a background vapor of Cd atoms at an estimated pressure of 10^{-11} torr. The average lifetime of an ion in the trap is several hours.

The axial secular oscillation frequency of an ion in the needle trap is given by

$$\omega_z = \sqrt{\frac{eU_0\eta}{mz_0^2} + \left(\frac{eV_0\eta}{\sqrt{2}m\Omega z_0^2}\right)^2} \quad (1)$$

under the pseudopotential approximation ($\omega_z \ll \Omega$) [16], where e is the charge and m the mass of the ion. The voltage efficiency factor η characterizes the reduction in trap confinement compared to the analogous quadrupole rf trap with hyperbolic electrodes of end cap spacing $2z_0$ and ring inner diameter $2\sqrt{2}z_0$ [16]. According to electrostatic simulations of the needle electrodes and grounded sleeves, $\eta = 0.17 \pm 0.01$ over the range of ion-electrode distances $z_0 = 23\text{--}250$ μm used in the experiment [17]. The axial secular oscillation frequency of a trapped $^{111}\text{Cd}^+$ ion is measured to be $\omega_z/2\pi = 2.77$ MHz for $U_0 = 0$ V, $V_0 \sim 600$ V at $z_0 = 136$ μm , consistent with simulations.

In order to measure the heating of ion motion in the trap, a single $^{111}\text{Cd}^+$ ion is first laser-cooled to near the ground state of motion through stimulated-Raman sideband cooling [11,18]. Doppler precooling prepares the ion in a thermal state with an average number of axial vibrational quanta $\bar{n} < 20$. Up to 80 cycles of pulsed sideband cooling

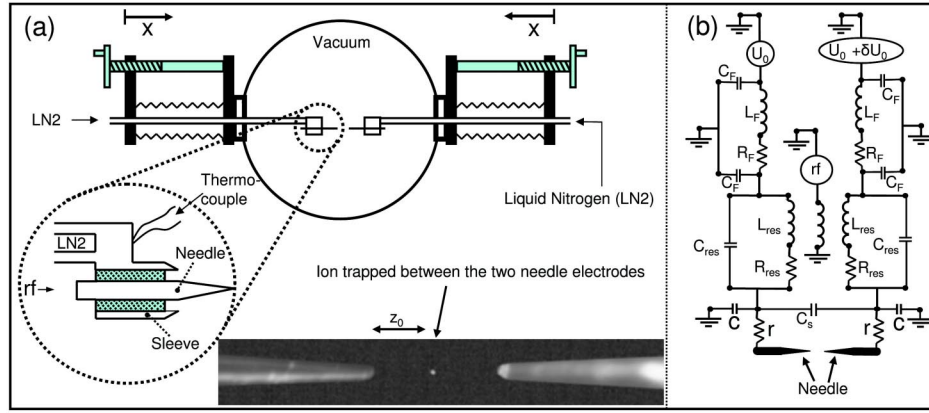


FIG. 1 (color online). (a) Schematic of double-needle rf ion trap. The needles are separated by variable distance $2z_0$ controlled by external translation stages. The needle tips are approximately spherical with a radius of $r_0 \approx 3 \mu\text{m}$ and supported by a conical shank of half-angle $\theta \sim 4^\circ$. Each surrounding cylindrical grounded sleeve of inner diameter 3.0 mm is recessed 2.3 mm from the needle tip and electrically isolated from the needles with an alumina tube. (b) Equivalent circuit for the ion trap, including a discrete model of the helical resonators providing rf potentials on each electrode. The rf resonators are independently biased with static potentials applied through π -network filters consisting of rf chokes of inductance $L_F = 100 \mu\text{H}$ and resistance $R_F = 3 \Omega$ between $C_F = 0.1 \mu\text{F}$ capacitors to ground. The outputs of the two rf resonators are shunted with a $C_S = 0.1 \mu\text{F}$ capacitor just outside of the vacuum feedthrough. The resistance of each electrode lead within the vacuum chamber is approximately $r \sim 0.1 \Omega$. Each needle electrode exhibits capacitance $C \sim 5 \text{ pF}$ to its grounded sleeve through the alumina spacer.

reduce the average occupation number to $\bar{n} < 0.3$. The value of \bar{n} is determined by measuring an asymmetric ratio in the strength of the stimulated-Raman first-order upper and lower sidebands, which is given by $\bar{n}/(1 + \bar{n})$ for a thermal state of motion [9,18]. We estimate that the systematic error in measuring \bar{n} is no more than 10%, from effects such as ion fluorescence baseline drifts, Raman laser intensity imbalances on the sidebands, and nonthermal vibrational distributions. Motional heating is measured by inserting a delay time (up to $\tau = 50 \text{ ms}$) after Raman cooling but before the sideband asymmetry probe. The heating rate $\dot{\bar{n}}$ of trapped ion motion is then extracted from the slope of $\bar{n}(\tau)$, as shown in Fig. 2. The linear growth of \bar{n} is consistent with the reasonable assumption that the temperature of the heat reservoir is much higher than the temperature of the ion [5], and the time scale for the ion to reach equilibrium is much longer than the measurement time (e.g., for a reservoir at temperature 300 K, it would take several hours for the ion to reach equilibrium). The heating rate of secular motion is related to the power spectrum of electric field noise $S_E(\omega) \equiv \int_{-\infty}^{\infty} \langle E(t)E(t+t') \rangle e^{i\omega t'} dt'$ at the position of the ion by [9]

$$\dot{\bar{n}} = \frac{e^2}{4m\hbar\omega_z} \left[S_E(\omega_z) + \frac{\omega_z^2}{2\Omega^2} S_E(\Omega \pm \omega_z) \right]. \quad (2)$$

The second term represents the cross coupling between the noise fields and the rf trapping fields to lowest order in the pseudopotential approximation [5,9,16].

Measurements of ion heating rate are presented in Fig. 3 at various trap frequencies ω_z for a fixed ion-electrode spacing of $z_0 = 103 \mu\text{m}$. In this data set, the trap strength is varied by applying different static potentials U_0 while

the rf potential amplitude is held constant at $V_0 \approx 600 \text{ V}$, with an exception for the point at $\omega_z/2\pi = 4.55 \text{ MHz}$, where $V_0 \approx 700 \text{ V}$. The data indicate that the heating rate decreases with trap frequency as $\dot{\bar{n}} \sim \omega_z^{-1.8 \pm 0.2}$, or equivalently that the electric field noise spectrum scales as $S_E(\omega) \sim \omega^{-0.8 \pm 0.2}$. Overall, these heating rates are similar to previous measurements in other Cd^+ traps of similar size and strength [11], and anomalously higher than the level of heating expected from thermal Johnson noise.

The two needle electrodes are wired to independent but identical circuits [Fig. 1(b)], and the Johnson noise from the resistive elements of the electrode circuits can be easily estimated. A circuit model with discrete elements is justified because the wavelength of the relevant time-varying

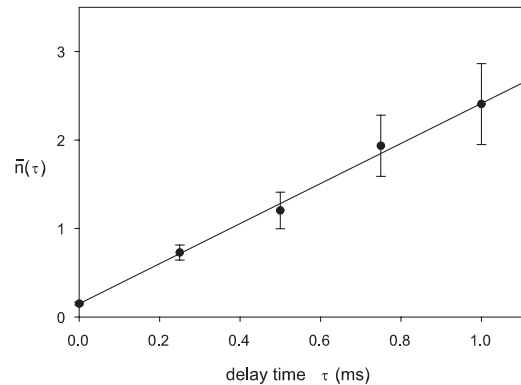


FIG. 2. Average thermal occupation number \bar{n} measured after various amounts of delay time τ . The axial trap frequency is $\omega_z/2\pi = 2.07 \text{ MHz}$ with an ion-electrode spacing of $z_0 = 64 \mu\text{m}$. The linear growth in time indicates a motional heating rate of $\dot{\bar{n}} = 2260 \pm 210 \text{ quanta/s}$.

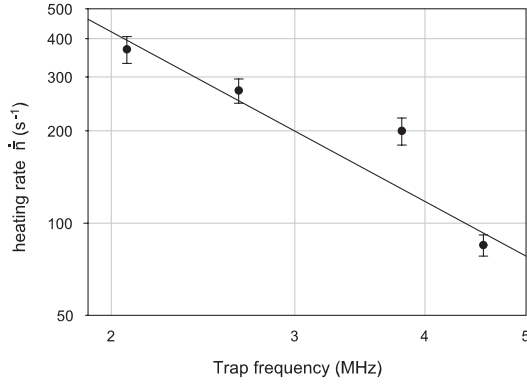


FIG. 3. Measured axial heating rate \dot{n} as a function of axial motional trap frequency ω . For these data, the ion-electrode spacing is fixed at $z_0 = 103 \mu\text{m}$ and the trap strength is varied by changing only the static potential U_0 while fixing V_0 , except for the highest frequency point where V_0 is 15% higher. The line is a fit to a power law, yielding $\dot{n} \sim \omega^{-1.8 \pm 0.2}$, implying that the electric field noise spectral density varies roughly as $S_E(\omega) \sim \omega^{-0.8 \pm 0.2}$ over this frequency range.

fields is much larger than the trap structure [5]. The net voltage noise $S_V(\omega)$ across the needle electrodes is simply an incoherent sum of all sources of Johnson noise $4k_B T_i R_i$ from each resistor R_i at temperature T_i in the circuit, where k_B is Boltzmann's constant. We also assume that the Johnson noise from each resistor is filtered by a shunt capacitor of value C_i , resulting in the expression

$$S_V(\omega) = \sum_i \frac{8k_B T_i R_i(\omega)}{1 + R_i(\omega)^2 C_i^2 \omega^2}. \quad (3)$$

This voltage noise gives rise to an electric field noise at the ion $S_E(\omega) = (\epsilon/2z_0)^2 S_V(\omega)$, where the geometrical efficiency factor $\epsilon \approx 0.7$ (determined by electrostatic modeling of the trap geometry) relates a given potential difference across the needle gap $2z_0$ to the resulting electric field at the ion position.

From the circuit model in Fig. 1(b), we consider three contributions to thermal Johnson noise. First, Johnson noise at frequency ω_z is directly driven by the series resistance of the needle electrode tips having negligible shunt capacitance ($C_1 \sim 0$). This resistance is estimated to be $R_1(\omega_z) = r = \rho/(\pi r_0 \tan\theta) \approx 0.1 \Omega$, where ρ is the resistivity of the electrode material at $T_1 = 300 \text{ K}$, r_0 is the needle-tip radius assumed to be much smaller than the skin depth multiplied by $\tan\theta$, and θ is the half-cone angle of the conical shank. Second, a somewhat smaller level of Johnson noise is estimated from the upstream rf choke of resistance $R_2(\omega_z) = R_F \sim 3 \Omega$ at $T_2 = 300 \text{ K}$, attenuated by filter capacitance $C_2 = C_F + C_S = 0.2 \mu\text{F}$ as shown in Fig. 1(b). Third, Johnson noise at the rf sideband frequencies $\Omega \pm \omega_z$ is dominated by the large effective resistance of the resonator circuit $R_3(\Omega \pm \omega_z) \approx (\Omega/2\omega_z)^2 R_{\text{res}}$ [5], where $R_{\text{res}} \sim 0.1 \Omega$ is the dc series resistance of the $T_3 = 300 \text{ K}$ resonator. But this near-resonant enhancement is

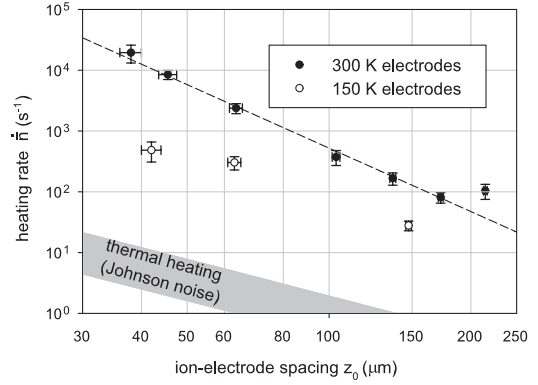


FIG. 4. Axial heating rate \dot{n} as a function of distance z_0 from trapped ion to each needle electrode, for warm and cold electrodes. The solid points are measured for 300 K electrodes, and the trap frequency is $\omega_z/2\pi = 2.07 \text{ MHz}$ for this data, with the rf and static trapping potentials increased as the trap is made larger. The measurements fit well to a scaling of heating rate with trap dimension of $\dot{n} \sim z_0^{-3.5 \pm 0.1}$ (dashed line). The lower set of measurements (open points) are acquired with the needle electrodes cooled to approximately 150 K through contact with a liquid nitrogen reservoir. These three points were measured on the same trapped ion at a trap frequency of $\omega_z/2\pi = 2.07 \text{ MHz}$. (The $z_0 = 42 \mu\text{m}$ cold measurement was performed at $\omega_z/2\pi = 4.9 \text{ MHz}$ and has been scaled upward by a factor of ~ 3 to the expected heating rate at $\omega_z/2\pi = 2.07 \text{ MHz}$.) The shaded band at bottom, scaling as z_0^{-2} , is the expected range of heating from thermal Johnson noise in the trap circuitry.

offset by the $(\omega_z/\Omega)^2$ term in Eq. (2), and moreover, because the resulting noise is heavily suppressed by the resonator shunt capacitor $C_3 = C_S = 0.1 \mu\text{F}$, this source of noise can be neglected compared to the others [19]. In sum, we expect a thermal Johnson noise heating rate of $\dot{n} \sim (200/z_0)^2 (\omega_z/2\pi)^{-1} \text{ s}^{-1}$ at 300 K, where z_0 is expressed in μm and $\omega_z/2\pi$ in MHz. At an electrode temperature of $T_1 = 150 \text{ K}$ ($T_2 = T_3 = 300 \text{ K}$), we expect the heating rate from Johnson noise to be ~ 6 times lower, including a factor of 3 reduction in the resistivity of the tungsten electrodes.

Figure 4 shows several measurements of heating rates at various values of the distance z_0 between the ion and the needle electrodes. This represents the first controlled measurement of heating as a function of electrode proximity, without requiring a comparison across different trap structures, electrode materials, surface qualities, or other factors. In these measurements, the axial trap frequency is held to $\omega_z/2\pi = 2.07 \text{ MHz}$ by varying both the rf and static potentials V_0 and U_0 as the needle spacing is changed [20]. As seen in the figure, the heating rate fits well to a power law, scaling as $\dot{n} \sim z_0^{-3.5 \pm 0.1}$, and is again much higher than that expected from thermal Johnson noise. The observed anomalous heating is thought to originate from fluctuating patch potentials on the electrode surfaces, and the scaling of this heating with electrode proximity provides information regarding the spatial size of pre-

sumed patches. For a single microscopic patch on the needle electrodes (spatial size much smaller than z_0), the electric field noise (e.g., heating rate) is expected to scale as z_0^{-4} . For uniformly distributed microscopic patches on the needle electrodes, the electric field noise is expected to scale between z_0^{-2} and z_0^{-4} , depending on the details of the electrode geometry. On the other hand, correlated noise across the entire electrode structure (e.g., from thermal Johnson noise or applied voltage noise) is expected to produce a heating rate that scales as z_0^{-2} . The observed $z_0^{-3.5 \pm 0.1}$ scaling rules out correlated noise on the electrodes and is consistent with a model of microscopic patches much smaller than the ion-electrode spacing z_0 . (It is difficult to ascertain the precise average patch size without detailed knowledge of the patch distribution on the electrodes.)

We repeat the measurement of axial motional heating of a trapped ion at various values of z_0 , but this time with the needle electrodes cooled via contact with a liquid nitrogen reservoir. While the electrode mount is measured to be 80 ± 5 K with a vacuum thermocouple, the needle tip is significantly hotter due to absorption of blackbody radiation at 300 K and the limited heat conduction from the very narrow needle electrode to the mount. We measure the shank of the needle to be 120 K, and we estimate that the needle tips are cooled to a temperature of 150 ± 20 K. The measured heating rates for cold trap electrodes is plotted in the lower set of data in Fig. 4. These three measurements were performed on one and the same $^{111}\text{Cd}^+$ ion, over a 6-h period. The measured heating rate with cold electrodes is still higher than that expected from Johnson noise by about 2 orders of magnitude, as shown in the figure. However, the nonlinear dependence of observed ion heating with electrode temperature is clear. The ion heating rate is suppressed by an order of magnitude for a decrease in electrode temperature by only a factor of 2, suggesting that the anomalous heating observed in ion traps may be thermally driven and activated at a threshold temperature, and that further cooling to 77 K or lower may even quench this anomalous heating completely.

We acknowledge useful discussions with J. A. Rabchuk and assistance from P. C. Haljan, P. J. Lee, and J. Li. This work is supported by the NSA and DTO under ARO Contract No. W911NF-04-1-0234 and the NSF ITR Program.

*Electronic address: crmonroe@umich.edu

[1] V. Meyer *et al.*, Phys. Rev. Lett. **86**, 5870 (2001).

- [2] P. O. Schmidt *et al.*, Science **309**, 749 (2005).
 [3] M. A. Rowe *et al.*, Nature (London) **409**, 791 (2001); D. L. Moehring *et al.*, Phys. Rev. Lett. **93**, 090410 (2004).
 [4] J. I. Cirac and P. Zoller, Phys. Rev. Lett. **74**, 4091 (1995).
 [5] D. J. Wineland *et al.*, J. Res. Natl. Inst. Stand. Technol. **103**, 259 (1998).
 [6] K. Mølmer and A. Sørensen, Phys. Rev. Lett. **82**, 1835 (1999); G. J. Milburn, S. Schneider, and D. F. V. James, Fortschr. Phys. **48**, 801 (2000).
 [7] C. A. Sackett *et al.*, Nature (London) **404**, 256 (2000); H. Häffner *et al.*, Nature (London) **438**, 643 (2005); D. Leibfried *et al.*, Nature (London) **438**, 639 (2005).
 [8] F. Schmidt-Kaler *et al.*, Nature (London) **422**, 408 (2003); J. Chiaverini *et al.*, Science **308**, 997 (2005); K.-A. Brickman *et al.*, Phys. Rev. A **72**, 050306(R) (2005).
 [9] Q. A. Turchette *et al.*, Phys. Rev. A **61**, 063418 (2000).
 [10] S. K. Lamoreaux, Phys. Rev. A **56**, 4970 (1997); D. F. V. James, Phys. Rev. Lett. **81**, 317 (1998); C. Henkel and M. Wilkens, Europhys. Lett. **47**, 414 (1999).
 [11] L. Deslauriers *et al.*, Phys. Rev. A **70**, 043408 (2004).
 [12] D. Kielpinski, C. Monroe, and D. Wineland, Nature (London) **417**, 709 (2002); M. A. Rowe *et al.*, Quantum Inf. Comput. **2**, 257 (2002); J. P. Home and A. M. Steane, quant-ph/0411102; W. K. Hensinger *et al.*, Appl. Phys. Lett. **88**, 034101 (2006); D. Stick *et al.*, Nature Phys. **2**, 36 (2006).
 [13] M. Blencowe and Y. Zhang, J. Appl. Phys. **91**, 4249 (2002); J. M. Martinis *et al.*, Phys. Rev. B **67**, 094510 (2003); O. Astafiev *et al.*, Phys. Rev. Lett. **93**, 267007 (2004); F. C. Wellstood, C. Urbina, and J. Clarke, Appl. Phys. Lett. **85**, 5296 (2004).
 [14] J. B. Camp, T. W. Darling, and R. E. Brown, J. Appl. Phys. **69**, 7126 (1991).
 [15] C. A. Schrama *et al.*, Opt. Commun. **101**, 32 (1993).
 [16] H. G. Dehmelt, Adv. Atom. Mol. Opt. Phys. **3**, 53 (1967).
 [17] Without the grounded sleeves, simulations predict that the voltage efficiency factor drops to $\eta \sim 0.06$, as the effective ground electrode is several cm away from the needles. This is consistent with measurements of the trap frequency in an earlier (sleeveless) version of the trap.
 [18] C. Monroe *et al.*, Phys. Rev. Lett. **75**, 4011 (1995).
 [19] For “symmetric” trap designs where the rf electrodes symmetrically surround the ion and are wired together, the resulting common-mode thermal Johnson noise from the rf leads should vanish due to symmetry.
 [20] Previous measurements of axial heating of trapped Cd^+ ions in a linear trap [11] show no correlation between the heating rate and the rf trapping voltage amplitude V_0 . These earlier measurements were performed over similar ranges of rf voltages and trap frequencies as used for the current experiment. We therefore assume that the origin of anomalous heating measured for the needle trap is not directly influenced by the rf voltage amplitude.